Journal of Applied Polymer Science

Silver-Releasing and Antibacterial Activities of Polyphenol-Based Polyurethanes

Jia Chen, Ying Peng, Zhen Zheng, Peiyu Sun, Xinling Wang
School of Chemistry and Chemical Engineering, State Key Laboratory of Metal Matrix Composites, Shanghai Jiao Tong University, Shanghai 200240, China
Correspondence to: X. Wang (E-mail: xlwang@sjtu.edu.cn)

ABSTRACT: Inspired by mussel adhesive proteins, catechol functional groups play an important role in the ability of the mussel to adhere to organic and inorganic surfaces. A novel functional polyurethane (PU) based on hydrolysable tannins that contain a number of catechol groups was successfully synthesized and characterized. These catechol groups were used as a reducer for Ag (I) to form Ag (0), and to prepare polyurethane/silver nanoparticles composites. These kinds of polyurethane containing Ag nanoparticles showed obvious inhibition of bacterial growth because of the conjunct actions of the well-known antibacterial property of silver and the anti-fouling property of PEG. It is possible for these materials to be applied widely into antibacterial adhesive coatings for surface modification due to their low cost and the material-independent adhesive property of catechol groups in tannins. © 2014 Wiley Periodicals, Inc. J. Appl. Polym. Sci. **2015**, *132*, 41349.

KEYWORDS: coatings; composites; nanoparticles; nanowires and nanocrystals; polyurethanes

Received 7 June 2014; accepted 31 July 2014
DOI: 10.1002/app.41349

INTRODUCTION

Infection is a major medical theory associated closely with health care environments. Literatures report the existence of relatively high (5–10%) incidence of infections for patients.[1,2] In the study of Spelman,[1] the sources and modes of transmission of pathogenic bacteria have been summarized. The sources signed as "inanimate hospital environment" and "hospital equipment" includes diverse items such as cell phones, pagers, computer keyboards, doorknobs, and others. Modes of transmission of pathogenic bacteria occur in various approaches such as touching, coughing, sneezing or other reactions. Such circumstances are common under nosocomial conditions where the transmission of pathogenic bacteria is feared because of the continually increasing resistance to antibiotics.

The most common method to thwarting the spread of infection is the direct addition of a biocide to the polymer material.[3–6] A normal method to conferring biocidal action is the modification or coating of a solid surface so that the biocide is bonded to the surface. The bound of biocidal materials is various and includes such as metal salts of silver, antibiotics, phenols and iodine. Several groups have modified existing surfaces with biocides.[7–10]

The mussel adhesive proteins (MAPs) contain unusually high content of catechol functional groups and are capable of adhesion to most organic and inorganic surfaces. Recent work from Dominic et al. has demonstrated redox coupling between DOPA-modified polymers and Ag (I) metal ions, leading to the formation of Ag nanoparticles via catechol oxidation.[11,12] According to Deming et al.,[13] the catechol groups in DOPA play a key role in the universal adhesion property because of their chemical versatility and diversity of affinity, while the former reports have shown the use of Ag (I) as an oxidizing agent for catechol groups.[14,15] Silver nitrate used as an oxidant was mixed with polyurethane and deoxidized by catechol groups in dopamine leading to formation of Ag (0), which is an easy reaction without any activator. However, despite the excellent chemical properties of dopamine, the application of dopamine in biocidal polymer materials is limited by its high cost.[16] It is significant for wide application to find other commonly raw materials to replace the dopamine.

Tannins are kinds of relatively cheap natural-source compounds with a large number of catechol functional groups, which are widely spread in plants and foods of plant origins, particularly in fruits, legume seeds, cereal grains and different beverages. The compositions of tannins are very complex and usually divided into the hydrolysable tannins and proanthocyanidins (PAs). Hydrolysable tannins are esters of phenolic acids and polyols, while PAs, forming the second group of tannins, are far more common on our diet.[17]

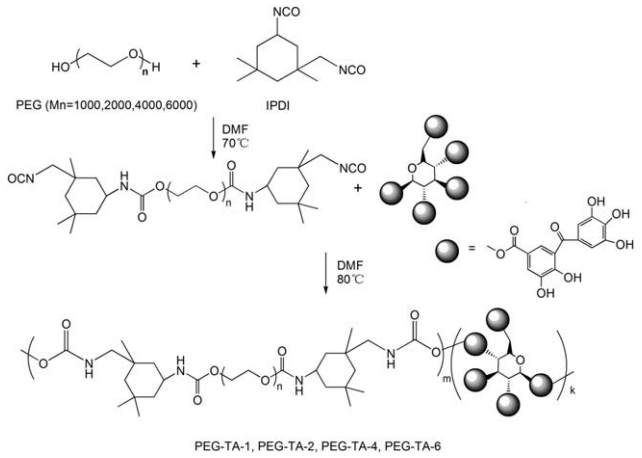

Scheme 1. Synthesis of polyurethane containing tannin.

In previous reports on surface modifiers, most attached effective compounds to glass or polymer surfaces. In this article, we plan to prepare one kind of polymer material, which is easily prepared, low cost and effectively antibacterial. Because of its wide availability, low cost, and excellent physical and biological properties, polyurethane (PU) has become one of the most versatile polymers in medical, industrial, adhesion, coating, and environmental applications.[18,19] Following prior work that has shown the biocidal efficacy of the modified polyurethane, it's possible to prepare a novel functional polyurethane containing tannins which also owns the antibacterial activity. The presence of Ag (I) ions, as a precursor for Ag nanoparticle, induces the coating containing tannins cross-linking via the oxidation of catechol groups and imparts the antibacterial activity to the polymer coating.

EXPERIMENTAL

Materials

Polyethylene glycol (PEG, $M_n = 1000$, 2000, 4000, 6000) from Sinopharm Chemical Reagent was dehydrated for 2 h at 90–95°C. Tannin (TA, $M_n = 1701.20$) from TCI (Shanghai) Development was dehydrated at 110°C for 3 h. The 3-isocyanatomethyl-3,5,5-trimethylcyclohexyl isocyanate (IPDI) from Bayer (Shanghai), stannous octoate ($Sn(Oct)_2$) from Sigma–Aldrich (Shanghai) and silver nitrate ($AgNO_3$, 99.8%) from Sinopharm Chemical Reagent were used without further purification. *N*,*N*-dimethylformamide (DMF) from Sinopharm Chemical Reagent was dried before use. Phosphate buffered saline (PBS) was prepared by dissolving 7.9 g NaCl, 0.2 g KCl, 0.24 g KH_2PO_4, and 1.44 g Na_2HPO_4 into 900 mL deionized water. Its pH was adjusted to 7.40 with 1 *M* NaOH aqua or 1 *M* HCl aqua. Then the solution was mixed with additional water to 1 L in a volumetric flask. Bacteria strains *Staphylococcus aureus* (ATCC 6538) and *Escherichia coli* (ATCC 8739) were purchased from Shanghai Fu Xiang Biological Technology. Tryptic soy agar and tryptic soy broth were obtained from Shanghai Zhi Yan Biological Technology.

Synthesis of Series of PEG-TA

A series of polyurethane (PU) samples were synthesized by a two-step method (Scheme 1) as previous report.[20] (The synthesized PU was generally referred as PEG-TA. In detail, the samples were named as PEG-TA-1, PEG-TA-2, PEG-TA-4, PEG-TA-6, respectively corresponding to the M_n of the PEG, which were 1000, 2000, 4000, 6000). Under the protection of nitrogen (N_2), PEG ($M_n = 1000$, 2000, 4000, 6000) and IPDI were added to 40 g dried DMF in the molar ratio of OH : NCO = 1 : 2 (Table I) and were allowed to react for 3 h at 70°C in the presence of $Sn(Oct)_2$ as a catalyst.[21] Excess tannin (8.5 g) was added to the solution and the reaction was allowed to continue at 80°C for another 24 h. After reaction, the final system was precipitated in ether. The PEG-TA samples were filtered, washed several times, and dried at 70°C for 3 days in a vacuum prior to any characterization. Taking PEG-TA-1 as an example, the NMR analysis was shown in Figure 1. The chemical shifts at 9.32 and 9.01 ppm corresponded to protons of the —OCO—NH—CH— and —OCO—NH—CH_2— moieties.

Table I. Composition of the PEG-TA Samples

Samples	OH : NCO	PEG M_n	PEG g	IPDI (g)	Tannin (g)	$Sn(Oct)_2$ (wt %)
PEG-TA-1	1 : 2	1000	5	2.22	8.5	0.1
PEG-TA-2	1 : 2	2000	10	2.22	8.5	0.1
PEG-TA-4	1 : 2	4000	20	2.22	8.5	0.1
PEG-TA-6	1 : 2	6000	30	2.22	8.5	0.1

Preparation of PEG-TA Coatings

Blank substrates (Ti, Fe, glass, 10 mm × 10 mm) were sterilized in ethanol for three times. Coatings were prepared by dipping blank substrates in a THF solution containing 30 mg mL^{-1} PEG-TA for 24 h, then washed three times with deionized water, and dried at room temperature for at least 3 days before any characterization.

Preparation of Antimicrobial Coatings

All substrates coated with PEG-TA samples were dipped in 8.5 mg mL^{-1} $AgNO_3$ in dark room for 24 h, then washed three times with deionized water, and dried at room temperature for at least 3 days before any characterization.

Characterization of the Release of Ag(0)

The UV–vis Spectrum performed on a Perkin Elmer Lambda 20 was used to characterize of the release of Ag(0). For example, PEG-TA-1 and $AgNO_3$ solutions were freshly prepared before use. The sample that 50 μL of 20 mg mL^{-1} PEG-TA-1 solution in THF added into 2694 μL THF was blank, followed by addition of 306 μL of 8.5 mg mL^{-1} $AgNO_3$ solution in THF. The final solution was pipetted quickly until well mixed. The UV–vis characterization of Ag(0) was tested as soon as the addition of silver nitrate, then once every 3 min until 33 min.

TEM Characterization

Transmission electron microscopy (TEM) was recorded on a JEM-2100 to observe the load of silver nanoparticles on the PEG-TA coatings. The reaction system containing silver nitrate (previously used for the UV–vis test) of 5 μL was dropped on EM grids and was dried fully before analysis.

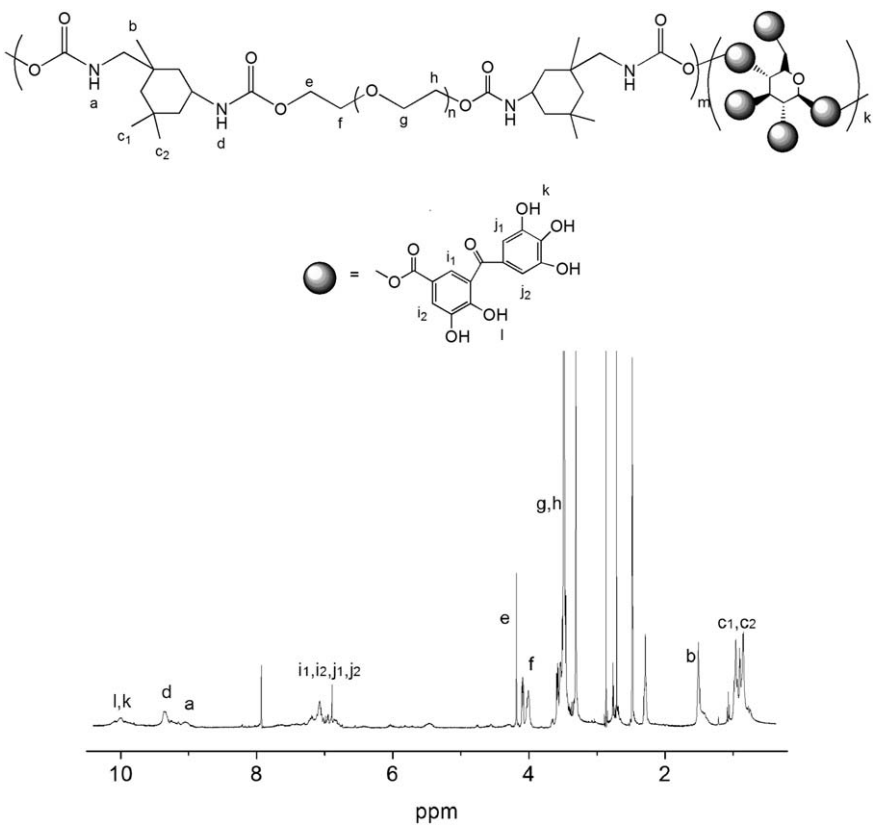

Figure 1. ^{1}H-NMR spectrum of PEG-TA-1.

Bactericidal Testing

A modified ATCC-100 biocidal testing protocol was employed. *E. coli* (ATCC 8739) and *S. aureus* (ATCC 6538) were grown in tryptic soy broth at 37°C for 14 h from previously frozen inoculums. All unmodified substrates and PEG-TA/Ag modified substrates were sterilized under UV irradiation for at least 30 min, and incubated at 37°C with 1 mL of phosphate buffered saline (PBS) containing $\sim 10^8$ CFU mL^{-1} colonies for 24 h. Substrates were fixed with glutaric dialdehyde (2.5%, 4°C) for 1–2 min and rinsed with PBS, then dried at room temperature. Attached bacteria were imaged by a scanning electron microscopy (SEM).

The antimicrobial activity of the coatings was tested by zone of inhibition (ZOI) to bacterial growth. Phosphate buffered saline (PBS) (200 μL) containing $\sim 10^6$ CFU mL^{-1} colonies were spread out on several blank agar plates, followed by putting the PEG-TA modified substrates and PEG-TA/Ag modified substrates on the middle of the plates. All the plates were incubated at 37°C for 12 h. The diameters of zone of inhibition (ZOI) to bacterial growth were measured.

The antimicrobial activity of the coatings was also determined by inhibition rate. A new suspension was prepared by centrifuging (7000 rpm, 10 min) from 30 mL of PBS containing $\sim 10^6$ CFU mL^{-1} colonies, followed by addition of 30 mL physiological saline (0.9% NaCl). Taking PEG-TA-1 as an example, PEG-TA-1 (20 mg) was dissolved in 5 mL new suspension into a test tube. By comparision, in another test tube containing 20 mg PEG-TA-1 and 5 mL new suspension, $AgNO_3$ solution was added according to the ratio of catechol/Ag(I) = 2/1. All PEG-TA samples were dealt like that. Put all test tubes into shaker ZHWY-2102C for another 18 h. Then 200 μL of final solutions from every tube were spread out on the blank agar plates and incubated at 37°C for 12 h. The surviving CFUs corresponding to the controlled and experimental samples (without or with $AgNO_3$) were counted respectively.

Other Characterizations

^{1}H-NMR spectra were obtained on an Advance-400 spectrometer (Bruker, Switzerland) in DMSO-d_6 at 25°C. The thermal behaviors of PEG-TA were examined by differential scanning calorimeter (DSC), TA Instrument Q2000 under a nitrogen atmosphere. Samples were heated from 40 to 120°C at a rate of 20°C min^{-1}, and kept for 10 min to eliminate the thermal history. The melt samples were then cooled to −80°C at 20°C min^{-1} and kept for 3 min, followed by heating to 120°C at 10°C min^{-1}. Thermo gravimetric analysis (TGA) was performed on a TA Instrument Q5000IR with a heating rate of 20°C min^{-1} from 40 to 600°C under a nitrogen atmosphere. Attenuated total reflection Flourier transformed infrared spectra (ATR-FTIR) were recorded on a Perkin-Elmer 1000 FTIR spectrometer. Contact Angles were determined by Contact Angle System OCA20. The surface chemical compositions were analyzed by a Shimadzu-Kratos (AXIS Ultra) X-ray photoelectron spectroscopy (XPS). The X-ray diffraction (XRD) was recorded on the Rigaku D/Max 2550 (Cu Kα, $\lambda = 1.5418$ Å).

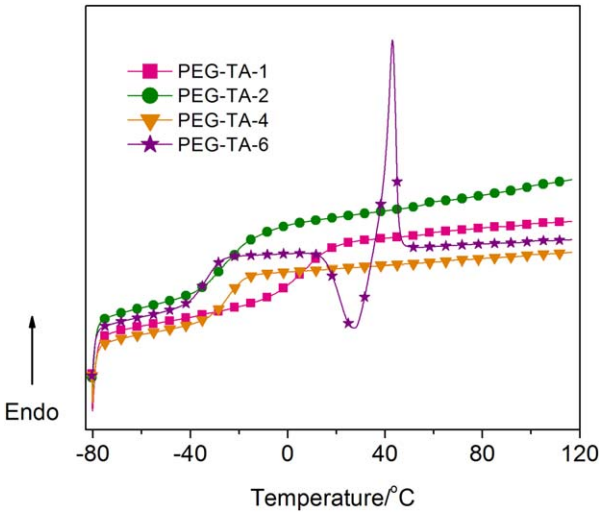

Figure 2. DSC curves of PEG-TA samples containing tannin. [Color figure can be viewed in the online issue, which is available at wileyonlinelibrary.com.]

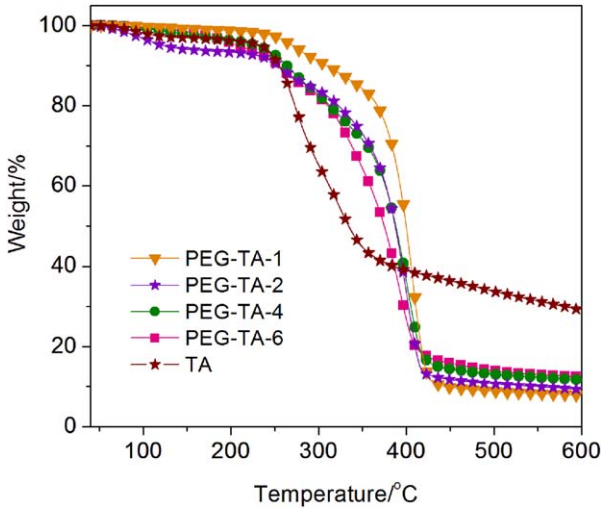

Figure 3. TGA curves of the pure tannin and PEG-TA samples containing tannin. [Color figure can be viewed in the online issue, which is available at wileyonlinelibrary.com.]

RESULTS AND DISCUSSION

Thermodynamic Properties of PEG-TA

DSC Analysis. DSC curves of the PEG-TA samples were shown in Figure 2. It was observed that all the PEG-TA samples except PEG-TA-6 showed only one glass transition temperatures (T_g), without melting points and crystallization transitions. The T_g of the PEG-TA samples depended on the content of tannin and soft segment, which increased from −34.1 to 6.4°C. This was mainly due to the higher backbone rigidity and higher chain interactions at higher tannin content.[22] Because of the higher chemical structural regularity of PEG6000, PEG-TA-6 showed a crystallization temperature at 42.9°C.

TGA Analysis. TGA curves of the pure tannin and PEG-TA samples containing tannin were shown in Figure 3. The curve of pure tannin showed only a two-step degradation; the first step occurred around 210°C, which was attributed to the degradation of the phenyl groups, and the second step occurred around 310°C, which was attributed to the degradation of the carbonyl groups.

However, all the curves of PEG-TA samples showed a three-step degradation process. The first step occurred around 220°C, which was attributed to the degradation of urethane bonds; nevertheless, a low concentration of IPDI resulted in an undetectable mass loss. The second step occurred in a similar temperature range (from 230 to 290°C), and was attributed to degradation of tannin. The third step occurred in the temperature range of 290–440°C, which was related to the degradation of the ester groups and the carbonyl groups of tannin. From the observed mass loss in the temperature range of the second degradation step, the content of tannin in each PEG-TA sample could be calculated (Table II).[23] The concentration of tannin increased from 26.5 to 35.9% with the increase of molecular weight of PEG, which was nearly consistent with the added amount of tannin. (In fact, "added tannin content" in Table II was the number of tannin really participating in chain extension, which cannot be accurately calculated merely from the molar of N═C═O in prepolymer because tannin is a compound with multiple functionalities.)

The DSC and TGA analysis confirmed the presence of tannin on the chain of the PU and the corresponding content of it.

Characterizations of PEG-TA Coatings

The PEG-TA samples containing tannin can attach to universal material surfaces because of the large amounts of catechol functional groups in tannin.

Table II. TGA Analysis of PEG-TA Samples Containing Tannin

	Second step		Third step				
Samples	Range temp (°C)	Loss mass (%)	Range temp (°C)	Loss mass (%)	Loss mass at second step (correct)	Calculated tannin content (%)	Added tannin content (%)
PEG-TA-1	224–285	8.9	285–436	80.2	9.0	26.5	27.8
PEG-TA-2	218–284	10.1	284–442	77.4	10.1	29.7	31.4
PEG-TA-4	219–291	11.0	291–439	68.3	11.2	32.9	35.6
PEG-TA-6	231–299	12.1	299–446	67.1	12.2	35.9	38.1
TA	210–307	33.0	307–366	22.3	34.0		

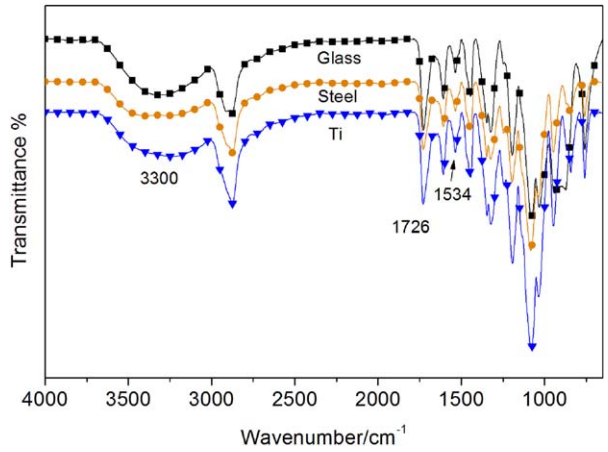

Figure 4. The ATR-FTIR spectra of different surfaces of substrates modified by PEG-TA-1. [Color figure can be viewed in the online issue, which is available at wileyonlinelibrary.com.]

ATR-FTIR Analysis. Taking PEG-TA-1 sample as an example, the ATR-FTIR spectra of different surfaces of substrates modified by PEG-TA-1 were shown in Figure 4. The peaks at 3300 and 1534 cm^{-1} were due to the N—H stretching vibration and deformation vibration, respectively. The peaks at 1726 cm^{-1} corresponded to the C═O stretching vibration. Bands at 2880, 1444, 1348, and 1320 cm^{-1} were attributed to the alkyl groups. And the peaks around 2250 cm^{-1} corresponding to N═C═O groups disappeared totally, indicating that the PEG-TA-1 sample was successfully synthesized. The similar peaks could be found on all the surfaces of substrates modified by all PEG-TA samples.

Contact Angle Analysis. Water contact angles of original and PEG-TA modified substrates were shown in Figure 5. The different original surfaces showed quite different water contact angles, while the different surfaces modified by the same PEG-TA sample showed similar water contact angles. The results indicated that PEG-TA samples owned the function to modify the surfaces by adhering to the substrates.

XPS Analysis. The high-resolution XPS spectra of O (1s) and C (1s) for PEG-TA-1 modified glass and unmodified glass substrates were shown in Figure 6. Quantitative analysis of XPS data for the two substrates was shown in Table III. The unmodified glass substrate exhibited stronger signals for silicon and oxygen, while weaker signal for carbon. The C (1s) spectra were further divided into three components, including C—C (284.7 eV), C—O (286.6 eV), C═O (288.2 eV). The C═O component was attributed to the side chain of tannin and oxidation. The large increase of the C—O component for the PEG-TA-1 modified substrate indicated the presence of the PEG ether carbons.[24] XPS analysis indicated the presence of PEG-TA sample on modified glass surface by adhering on the surface or effectively modifying the surface. The results are agreement with those of the ATR-FTIR spectra and water contact angles.

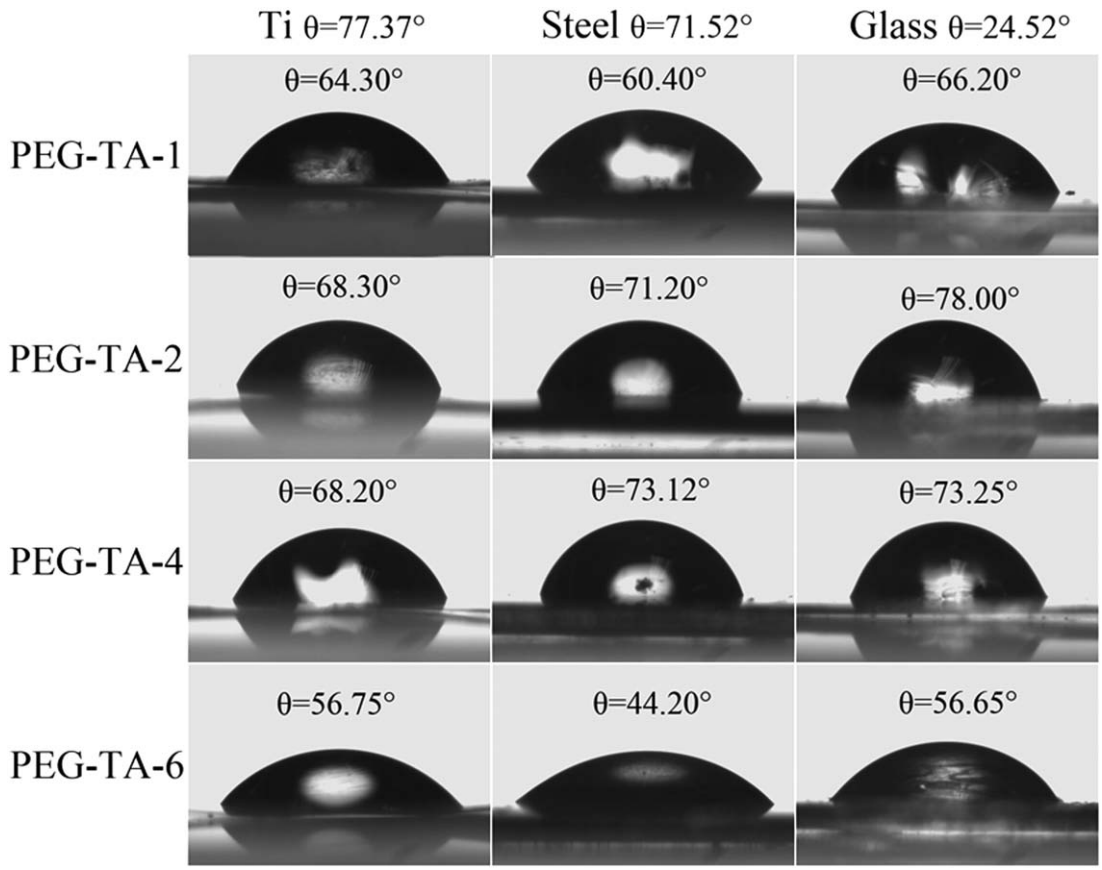

Figure 5. Water contact angles of original and PEG-TA modified substrates.

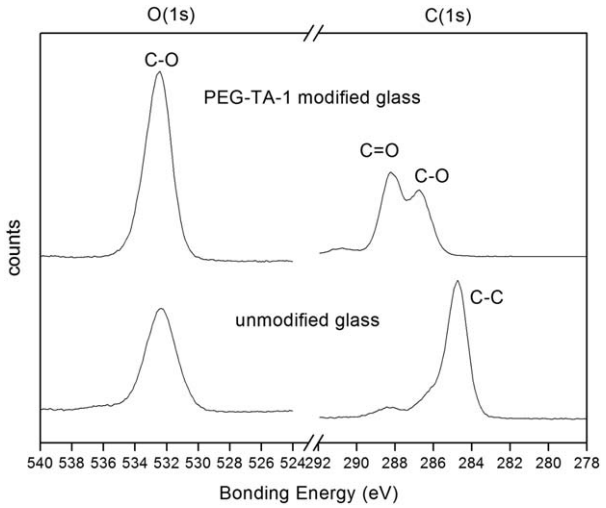

Figure 6. High-resolution XPS spectra of O (1s) (left) and C (1s) (right) of PEG-TA-1 modified and unmodified glass substrates.

Characterizations of Ag Nanoparticles

Characterization of the Release of Ag(0). UV–vis spectra were used to understand the release of silver particles as a consequence of the redox reaction of Ag (I) with PEG-TA samples, which were shown in Figure 7. That adding $AgNO_3$ to a THF solution of PEG-TA samples (catechol : Ag(I) = 2 : 1) resulted in the nearly instantaneous formation of silver particles and the observation of a yellow-brown stable solution. Their distributions were basically the same. Therefore, reaction of Ag (I) with PEG-TA-1 was systematically considered in this study. In Figure 7(a), corresponding to reaction times of 0–33 min, the arrow indicated the growth of absorbance at 430 nm with time, which was consistent with the release of silver particles.[12] Figure 7(b) showed the solution from Figure 7(a), which had reacted for 30 min and 2 days. It could be seen that the reaction continued slowly even after 30 min, and the maximum absorbance moved to around 400 nm by 2 days, possibly due to the surface plasmon resonance of metallic Ag nanoparticles caused by the collective excitation of the free electron gas or quinine groups of oxidized tannin.[25–28]

XRD Analysis. XRD was used to determine the nature of the particles on the PEG-TA/Ag films. Diffraction patterns of silver particles prepared by the reaction of Ag (I) with PEG-TA samples (catechol : Ag(I) = 2 : 1) were shown in Figure 8. Figure 8(a) showed diffraction characteristic peak of metallic Ag particles,[29] and indicated the ability of the PEG-TA-1 to stabilize the Ag particles. When the PEG-TA coatings were dipped into $AgNO_3$ aqueous solution for 24 h, their colors were changed from yellow to brown. Figure 8(b) pointed out the ability of redox reaction of Ag (I) was different with the change of the content of tannin in PEG-TA samples. However, no exact amount of Ag(0) could be drawn from these measurements because of the relatively low content of silver in comparison with the amorphous organic matrix.

Table III. Quantitative Analysis of XPS Data for Substrates

	Atomic concentration (atom%)				
Substrates	Si	O C—O, H_2O	C C=O	C—O	C—C, C—H
Unmodified glass	18.41 (102.79)	57.13 (532.13)	4.02 (288.23)	4.44 (286.71)	15.99 (284.73)
PEG-TA-1 modified glass	2.59 (102.63)	20.69 (532.46)	5.09 (288.33)	26.16 (286.63)	45.47 (284.83)

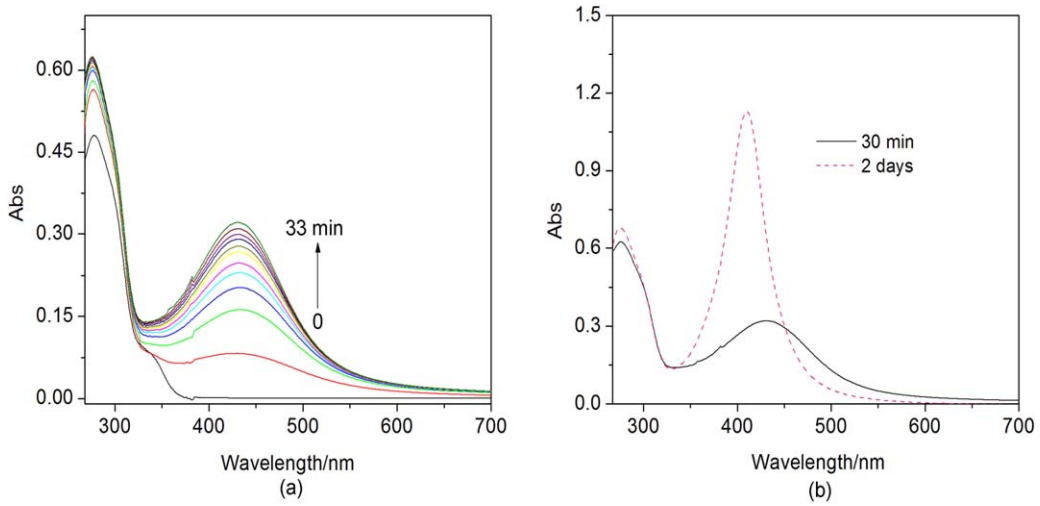

Figure 7. Absorption spectra of silver particles. (a) Time-dependent UV–vis spectra of PEG-TA-1 sample and $AgNO_3$ (catechol : Ag(I) = 2 : 1); (b) Sample from (a), which had reacted for 30 min and 2 days, respectively. [Color figure can be viewed in the online issue, which is available at wileyonlinelibrary.com.]

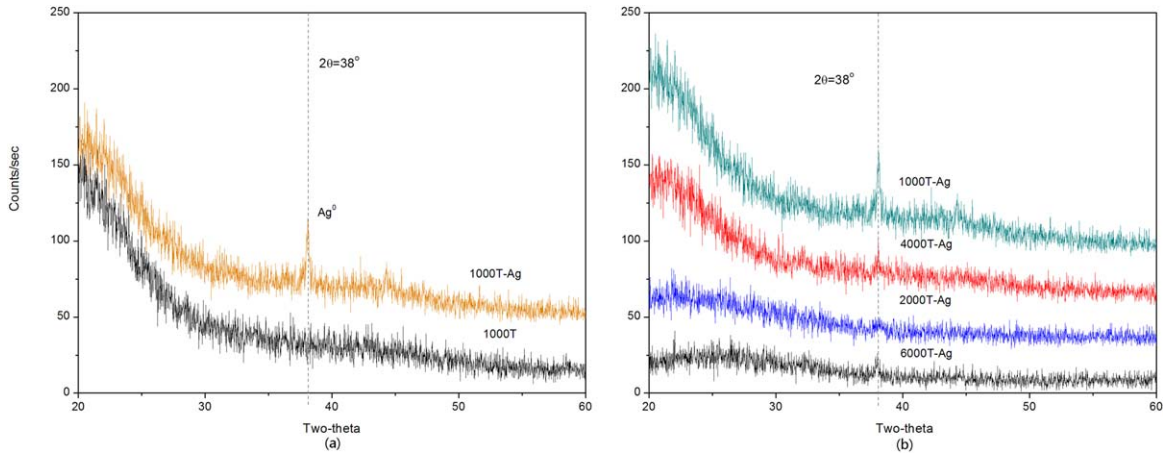

Figure 8. Diffraction patterns of silver particles prepared by the reaction of Ag (I) with PEG-TA samples (catechol : Ag(I) = 2 : 1). (a) Only with PEG-TA-1; (b) With all the PEG-TA samples. [Color figure can be viewed in the online issue, which is available at wileyonlinelibrary.com.]

TEM Analysis. The successful stabilization of silver nanoparticles by the PEG-TA samples was also confirmed by TEM. The schematic illustration of the formation of silver nanoparticles on PEG-TA films was shown in Figure 9(a). The shape and size distributions of Ag nanoparticles were detected. Figure 9(b) displayed images of nanoparticles obtained from the UV–vis study mentioned in Figure 7. The nanoparticles were mostly round-shaped and well-dispersed, with diameters up to 10 nm. This was perhaps due to the well-dispersed of catechol groups on the chain of the polymer.

Bacterial Viability and Attachment

The antibacterial activity of PEG-TA/Ag coatings was evaluated by measuring their ability to inhibit both Gram-positive (*S. aureus*) and Gram-negative (*E. coli*) bacteria for several times. Taking unmodified steel and PEG-TA/Ag modified steel as examples, the results were shown as Figure 10. After incubating in stock solution containing $\sim 10^8$ CFU mL^{-1} colonies for 24 h, bacterial colonies were clearly observed on the contact surface of the control steel, while there were bare colonies found on that of the PEG-TA/Ag modified steel.

The PEG-TA/Ag coatings exhibited a good inhibition rate. Shown as Figure 11, there were about $\sim 10^3$ CFUs on the plate for the PEG-TA coating, which was much lower than the original $\sim 10^6$ CFUs and was associated with the antifouling property of PEG. However, there were nearly no surviving CFUs on the plate for the PEG-TA/Ag coating, which was connected closely with the conjunct actions of the well-known antibacterial property of silver and the antifouling property of PEG, and the result further proved the existence of silver nanoparticles.

The PEG-TA/Ag coatings also exhibited a surrounding zone of inhibition (ZOI) to bacterial growth. Shown as Table IV, different PEG-TA/Ag samples showed different sizes (110–150% of the

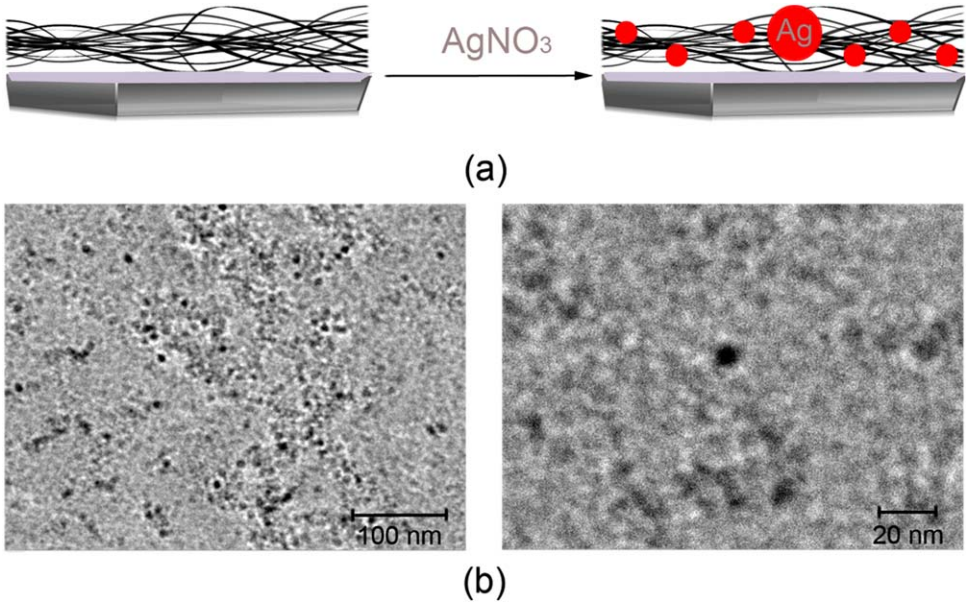

Figure 9. Catechol-mediated formation of silver nanoparticles on PEG-TA films. (a) Schematic illustration of the formation of silver nanoparticles on PEG-TA films; (b) TEM images of silver nanoparticles formed by reaction of Ag (I) with PEG-TA-1 (catechol : Ag (I) = 2 : 1). [Color figure can be viewed in the online issue, which is available at wileyonlinelibrary.com.]

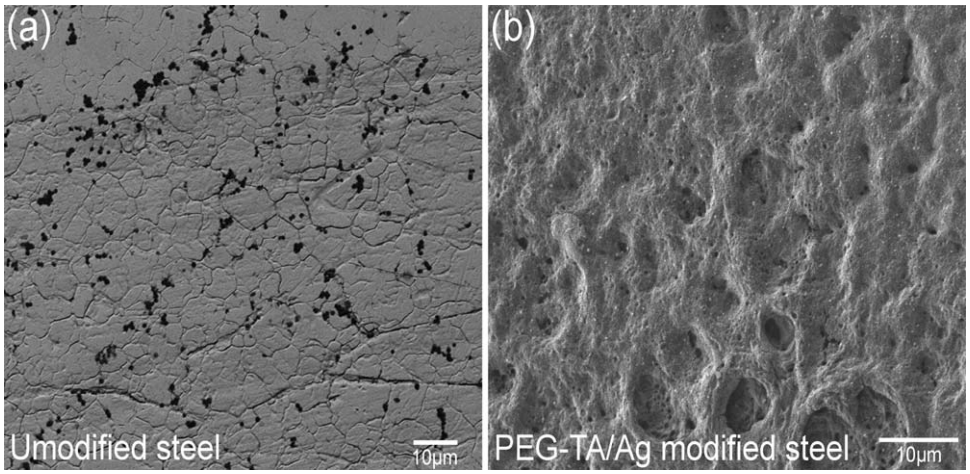

Figure 10. Representative scanning electron microscopy images of (a) unmodified steel and (b) PEG-TA/Ag modified steel exposed to *S. aureus* for 24 h.

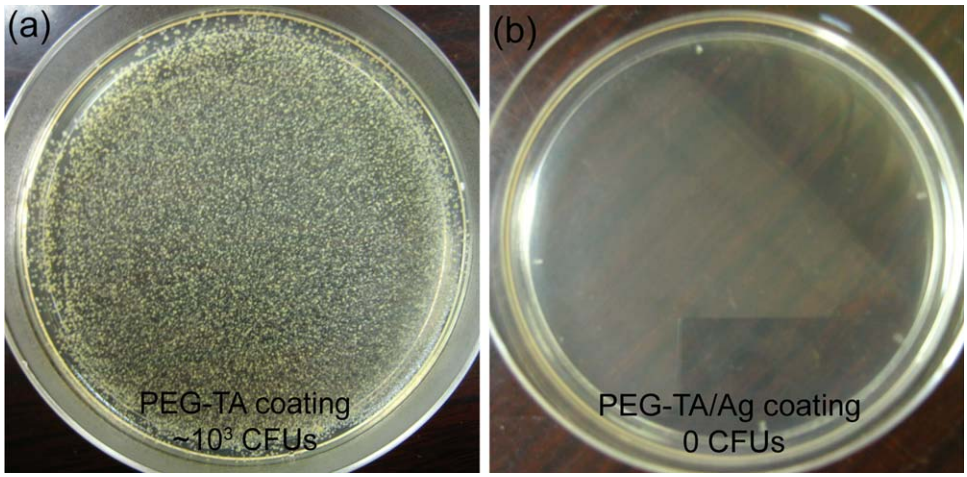

Figure 11. Bacterial attachment images of plates for (a) PEG-TA coating and (b) PEG-TA/Ag coating of the inhibition rate. The challenge was *S. aureus* and the incubation time was 12 h. [Color figure can be viewed in the online issue, which is available at wileyonlinelibrary.com.]

original diameter), which effectively controlled the bacterial growth. Moreover, Table IV also indicated that the antibacterial activity of coatings was mostly depended on the silver nanoparticles.

CONCLUSIONS

A series of antibacterial coatings were successfully synthesized through redox reactions between Ag (I) and catechol functional groups of polyurethane containing tannin. The DSC and TGA analysis confirmed the presence of tannin and the corresponding content of it. In this article, the role of catechol groups was to induce reduction of Ag (I) to Ag (0) as well as instill antibacterial property into polyurethane. With the ratio of catechol: Ag (I) = 2 : 1, the PEG-TA/Ag coatings were resistant to both Gram-negative bacteria and Gram-positive bacteria, which achieved 100% at 37°C after incubating for 12 h. In the future, this functional polyurethane may be widely used as functionalized antibacterial adhesive coatings for surface modification in the field of surface chemistry for its low cost and the material-independent adhesive property of catechol groups in tannin. Nevertheless, much remains to be learned about the adhesive

Table IV. Zone of Inhibition (ZOI) to Bacterial Growth of PEG-TA/Ag Coatings

Samples	PEG-TA-1	PEG-TA-1/Ag	PEG-TA-2/Ag	PEG-TA-4/Ag	PEG-TA-6/Ag
Original diameter (mm)	10	10	10	10	10
Zone of inhibition (mm) (*S. aureus*)	N/a	14.5 ± 0.3	12.6 ± 0.3	13.8 ± 0.7	11.1 ± 0.3
Zone of inhibition (mm) (*E. coli*)	N/a	15.3 ± 0.5	12.0 ± 0.5	12.7 ± 0.5	11.0 ± 0.5

The incubation time was 12 h.

strength, chemical stability and durability of the polyurethane containing tannin and the general efficacy of antibacterial coatings and materials.

ACKNOWLEDGMENTS

This work was supported by the Natural Science Foundation of China under Grant [21274085]; Shanghai Leading Academic Discipline Project under Grant [No. B202].

AUTHOR CONTRIBUTION

Xinling Wang contributed to the conception of the study; Jia Chen prepared the polyurethanes and the coatings, performed the data analyses and wrote the manuscript; Ying Peng contributed significantly to the synthesis, analysis and revise of manuscript; Zhen Zheng helped perform the analysis with constructive discussions; Peiyu Sun contributed to the instruction during the experiments.

REFERENCES

1. Spelman, D. W. *MJA* **2002**, *176*, 286.
2. Hacek, D. M.; Suriano, T.; Noskin, G. A.; Kruszynski, J.; Reisberg, B.; Peterson, L. R. *Am. J. Clin. Pathol.* **1999**, *111*, 647.
3. Woo, G. L. Y.; Mittelman, M. W.; Santerre, J. P. *Biomaterials* **2000**, *21*, 1235.
4. Woo, G. L. Y.; Yang, M. L.; Yin, H. Q.; Jaffer, F.; Mittelman, M. W.; Santerre, J. P. *J. Biomed. Mater. Res.* **2002**, *59*, 35.
5. Darouiche, R. O.; Green, G.; Mansouri, M. D. *Int. J. Antimicrob. Ag.* **1998**, *10*, 83.
6. Tiller, J. C.; Sprich, C.; Hartmann, L. *J. Control. Release.* **2005**, *103*, 355.
7. Tiller, J. C.; Liao, C.-J.; Lewis, K.; Klibanov, A. M. *Proc. Natl. Acad. Sci. USA* **2001**, *98*, 5981.
8. Tiller, J. C.; Lee, S. B.; Lewis, K.; Klibanov, A. M. *Biotechnol. Bioeng.* **2002**, *79*, 465.
9. Lin, J.; Qiu, S. Y.; Lewis, K.; Klibanov, A. M. *Biotechnol. Bioeng.* **2003**, *83*, 168.
10. Lee, S. B.; Koepsel, R. R.; Morley, S. W.; Matyjaszewski, K.; Sun, Y. J.; Russell, A. J. *Biomacromolecules* **2004**, *5*, 877.
11. Fullenkamp, D. E.; Rivera, J. G.; Gong, Y-K.; Lau, K. H.; He, L. H.; Varshney, R.; Messersmith, P. B. *Biomaterials* **2012**, *33*, 3783.
12. Black, K. C. L.; Liu, Z. Q.; Messersmith, P. B. *Chem. Mater.* **2011**, *23*, 1130.
13. Yu, M.; Hwang, J.; Deming, T. J. *J. Am. Chem. Soc.* **1999**, *121*, 5825.
14. Hackman, R. H.; Todd, A. R. *Biochem. J.* **1953**, *55*, 631.
15. Dyer, E.; Baudisch, O. *J. Biol. Chem.* **1932**, *95*, 483.
16. Rischka, K.; Richter, K.; Hartwig, A.; Kozielec, M.; Slenzka, K.; Sader, R.; Grunwald, I. In Biological Adhesive Systems; Byern, J.; Grunwald, I., Eds.; Springer Vienna: Vienna, **2010**; Chapter 13, p 201.
17. Santos-B. C.; Scalbert, A. *J. Sci. Food. Agric.* **2000**, *80*, 1094.
18. Oertel, G.; Abele, L. Polyurethane Handbook: Chemistry, Raw Materials, Processing, Application, Properties; Hanser Publishers: Munich, **1985**.
19. Szycher, M. Szycher's Handbook of Polyurethanes; CRC Press: Florida, **1999**.
20. Sarkar, D.; Yang, J.-C.; Gupta, A. S.; Lopina, S. T. *J. Biomed. Mater. Res. A* **2009**, *90*, 263.
21. Skarja, G. A.; Woodhouse, K. A. *J. Biomater. Sci. Polym. Edn.* **1998**, *9*, 271.
22. Liu, J.; Ma, D. Z. *J. Appl. Polym. Sci.* **2002**, *84*, 2206.
23. Peng, Y.; Zheng, Z.; Sun, P. Y.; Wang, X. L.; Zhang, T. K. *New J. Chem.* **2013**, *37*, 729.
24. Dalsin, J. L.; Lin, L. J.; Tosatti, S.; Vörös, J.; Textor, M.; Messersmith, P. B. *Langmuir* **2005**, *21*, 640.
25. Manna, A.; Imae, T.; Aoi, K.; Okada, M.; Yogo, T. *Chem. Mater.* **2001**, *13*, 1674.
26. Campbell, G. S. *Agr. Forest. Meteorol.* **1986**, *36*, 317.
27. Lee, B. P.; Dalsin, J. L.; Messersmith, P. B. *Biomacromolecules* **2002**, *3*, 1038.
28. Yamada, K.; Chen, T. H.; Kumar, G.; Vesnovsky, O.; Topoleski, L. T.; Payne, G. F. *Biomacromolecules* **2000**, *1*, 252.
29. Jette, E. R.; Foote, F. *J. Chem. Phys.* **1935**, *3*, 605.